

1  
2 **Supplementary Information:**  
3

4 **Wandering minds, sleepy brains:**  
5 **lapses of attention and local sleep in wakefulness.**  
6

7  
8 Thomas Andrillon<sup>1\*</sup>, Angus Burns<sup>1</sup>, Teigane MacKay<sup>1</sup>, Jennifer Windt<sup>2</sup> & Naotsugu  
9 Tsuchiya<sup>1,3,4</sup>

10  
11  
12 **Affiliations:**

- 13 1. School of Psychological Sciences, Turner Institute for Brain and Mental Health, Monash  
14 University, Melbourne 3168, Victoria, Australia.  
15 2. Philosophy Department, Monash University, Melbourne 3168, Victoria, Australia.  
16 3. Center for Information and Neural Networks (CiNet), National Institute of Information  
17 and Communications Technology (NICT), Suita, Osaka 565-0871, Japan  
18 4. Advanced Telecommunications Research Computational Neuroscience Laboratories, 2-  
19 2-2 Hikaridai, Seika-cho, Soraku-gun, Kyoto 619-0288, Japan.  
20

21  
22  
23 **Supplementary Methods**

24 **Supplementary Table 1**

25 **Supplementary Figures 1 to 3**  
26

## 27 **Supplementary Methods**

28 **Participants.** Prior to their participation in the protocol, all 26 participants but one filled in  
29 online surveys on Qualtrics (N=25). They reported normal levels of sleepiness (Epworth  
30 Sleepiness Scale:  $14.6 \pm 4.7$ ; mean  $\pm$  standard-deviation) and mind wandering (Mind  
31 Wandering Questionnaire<sup>1</sup>:  $3.6 \pm 0.91$ ) in their everyday lives.

32 **Experimental Design and Stimuli.** Face stimuli were divided in two parts vertically (half-left  
33 and half-right faces) which were flickered on the screen at different frequencies (12 and 15 Hz,  
34 counterbalanced across participants). Similarly, the digits were inserted in a Kanizsa illusory  
35 square (Fig. 1a) whose right and left parts also flickered at different frequencies (12 and 15  
36 Hz). This flickering was introduced to elicit Steady State Visual Evoked Potentials (SSVEPs)  
37 in the EEG signal. The detailed analysis of this aspect of our dataset will be reported elsewhere.  
38 As the flickering occurred at a high rate, participants did not report a negative effect on their  
39 ability to perform the SART.

40 **Experience Sampling.** Following task interruptions (probes), participants were asked to  
41 answer a series of 8 questions in the following fixed order: (1) 'Were you looking at the screen?'  
42 (response: yes / no); (2) 'Where was your attention focus?' (response: on-task / off-task / blank  
43 / don't remember); (3) 'What distracted your attention from the task?' (response: Something in  
44 the room / personal / about the task); (4) 'How aware were you of your focus?' (response: from  
45 1, I was fully aware, to 4, I was not aware at all); (5) 'Was your state of mind intentional?'  
46 (response: from 1, entirely intentional, to 4, entirely unintentional); (6) 'How engaging were  
47 your thoughts?' (response: from 1, not engaging, to 4, very engaging); (7) 'How well do you  
48 think you have been performing?' (response: from 1, not good, to 4, very good); (8) 'How alert  
49 have you been?' (response: extremely alert / alert / sleepy / extremely sleepy). Question 3 was

50 displayed only if participants answered off-task in question 1. In this report, we focus only on  
51 questions (2) and (8).

52 ***Physiological Recordings and Preprocessing.*** The raw pupil size was corrected for the  
53 occurrence of blinks as in 2. The timings of blinks were obtained through the EyeLink  
54 acquisition software. For each of these blinks, the pupil size was corrected by linearly  
55 interpolating the average signal preceding the blink onset ([-0.2, -0.1]s) and following the blink  
56 offset ([0.1, 0.2]s). The corrected signal was then low-pass filtered below 6Hz (two-pass  
57 Butterworth filter at the 4<sup>th</sup> order). Finally, for blinks longer than 2s, data points between -0.1s  
58 prior to blink onset and 0.1s after blink onset were considered missing.

59 ***Local Sleep.*** In sleep, according to established guidelines<sup>3</sup>, only waves with peak-to-peak  
60 amplitude exceeding 75 $\mu$ V are defined as slow waves. In wakefulness, previous studies relied  
61 on a relative rather than absolute threshold<sup>4-6</sup>. Here, we defined as slow-waves the waves with  
62 absolute peak-to-peak amplitude within the top 10% of all the waves detected for a given EEG  
63 electrode and a given participant. On average, the detection threshold was 30  $\mu$ V (average  
64 across N=26 participants and across all electrodes). Figure 3a shows the average waveform of  
65 the slow waves detected on electrode Cz as well as the average waveform of waves detected  
66 during sleep recording in another published dataset (N=15 participants)<sup>7</sup>. To compute the  
67 average waveform of sleep slow waves, we applied the same algorithm to epochs of 20s scored  
68 as NREM2 and NREM3. Only slow waves with peak-to-peak amplitude over 75 $\mu$ V were  
69 considered.

70 ***Drift Diffusion Modeling.*** The Drift Diffusion Model (DDM) proposes that a decision  
71 variable noisily accumulates evidence from a starting point ( $z$ ) with drift rate ( $v$ ) towards one  
72 of two boundaries that represent choice alternatives (i.e. ‘Go’ or ‘NoGo’; see Supplementary  
73 Figure 1). The decision threshold ( $a$ ) is the distance between the two boundaries and represents  
74 the amount of evidence that must be accumulated before a decision is made. Once the decision

75 variable crosses a decision boundary, a response is made. The DDM captures extra-decisional  
76 components, including stimulus encoding, response preparation and execution with the non-  
77 decision time parameter ( $t$ ). Five parameters were fitted using a DDM approach: the starting  
78 point ( $z$ ), drift rates for Go and NoGo responses ( $v_{Go}$  and  $v_{NoGo}$ ), the decision threshold ( $a$ ), the  
79 non-decision time parameter ( $t$ ). From the drift rates, we also extracted the drift rate bias ( $v_{Bias}$ ).  
80 Model selection was done using the Deviance Information Criteria (DIC), which assess  
81 goodness of fit while accounting for model complexity in hierarchical models<sup>8</sup>. Posterior  
82 predictive checks confirmed that the Go/No-Go DDM was able to reproduce the behaviour of  
83 our participants in our task. We simulated behaviour according to the DDM based on 100 draws  
84 from the posterior distributions for parameters. The model captured the key patterns of our  
85 behavioural data (Supplementary Figure 2; based on the Fz model), including a close matching  
86 of observed and predicted No-Go choice proportions as well as Go RT distributions.

87 **Statistics.** A cluster-permutation approach (derived from<sup>9</sup>) was applied to identify significant  
88 clusters in topographical maps. Significant clusters were defined as neighboring electrodes  
89 with a p-value below a threshold (called “cluster alpha”) of 0.01. For each cluster, we computed  
90 the sum of the t-values for all the electrodes belonging to the cluster (which we will refer to as  
91 the “cluster statistics”). We then created permuted datasets by permuting the labels of the  
92 predictor within each subject, each task and each electrode (N=1,000 permutations). For each  
93 of these permuted datasets, we also identified and retrieved the significant clusters and their  
94 cluster statistics. However, for each permutation, we retained only the cluster with the maximal  
95 absolute cluster statistics. Finally, for each real cluster of the real dataset, we compared their  
96 cluster statistics to the distribution of maximal cluster statistics obtained for the permuted  
97 datasets for positive and negative clusters separately. A Monte-Carlo p-value was derived from  
98 this comparison ( $p < 0.05$  means that a negative cluster has a cluster statistics below the 5<sup>th</sup>  
99 percentile of the permuted distribution and that a positive cluster has a cluster statistics above

100 the 95<sup>th</sup> percentile of the permuted distribution). In cases where several cluster-permutations  
101 were performed in the same analysis (Fig. 5 and 6), we corrected the Monte-Carlo p-values of  
102 the real clusters with the Bonferroni method.

103

#### 104 **References:**

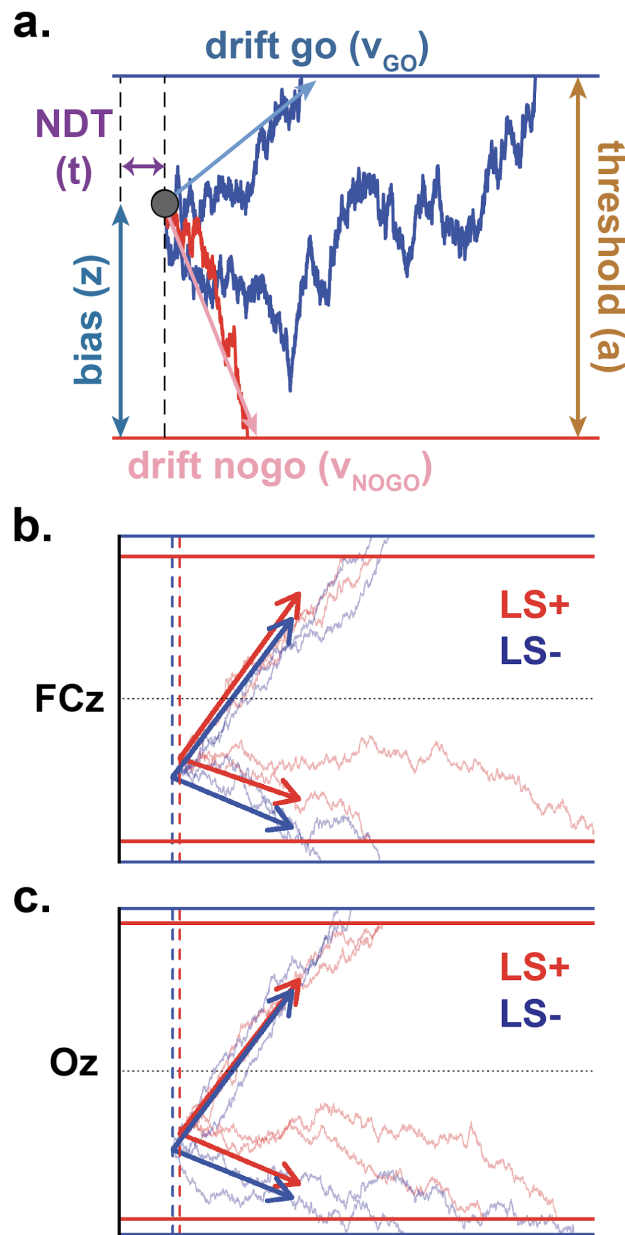
- 105 1. Mrazek, M. D., Phillips, D. T., Franklin, M. S., Broadway, J. M. & Schooler, J. W. Young  
106 and restless: validation of the Mind-Wandering Questionnaire (MWQ) reveals disruptive  
107 impact of mind-wandering for youth. *Frontiers in Psychology* **4**, (2013).
- 108 2. van Kempen, J. *et al.* Behavioural and neural signatures of perceptual decision-making are  
109 modulated by pupil-linked arousal. *eLife* **8**, (2019).
- 110 3. Iber, C., Ancoli-Israel, S., Chesson, A. & Quan, S. The AASM Manual for the Scoring of  
111 Sleep and Associated Events: Rules, Terminology and Technical Specifications. (2007).
- 112 4. Hung, C.-S. *et al.* Local experience-dependent changes in the wake EEG after prolonged  
113 wakefulness. *Sleep* **36**, 59–72 (2013).
- 114 5. Bernardi, G. *et al.* Neural and Behavioral Correlates of Extended Training during Sleep  
115 Deprivation in Humans: Evidence for Local, Task-Specific Effects. *Journal of*  
116 *Neuroscience* **35**, 4487–4500 (2015).
- 117 6. Quercia, A., Zappasodi, F., Committeri, G. & Ferrara, M. Local Use-Dependent Sleep in  
118 Wakefulness Links Performance Errors to Learning. *Frontiers in Human Neuroscience* **12**,  
119 (2018).
- 120 7. Legendre, G., Andrillon, T., Koroma, M. & Kouider, S. Sleepers track informative speech  
121 in a multitalker environment. *Nature Human Behaviour* **3**, 274–283 (2019).
- 122 8. Spiegelhalter, D. J., Best, N. G., Carlin, B. P. & van der Linde, A. Bayesian measures of  
123 model complexity and fit. *Journal of the Royal Statistical Society: Series B (Statistical*  
124 *Methodology)* **64**, 583–639 (2002).
- 125 9. Maris, E. & Oostenveld, R. Nonparametric statistical testing of EEG- and MEG-data. *J.*  
126 *Neurosci. Methods* **164**, 177–190 (2007).
- 127

128 **Supplementary Table 1. Summary of Linear Mixed-Effects Models**

Figure	Predicted Variable X	Level	Predictor Of Interest	Model 0	Model 1
2b	false alarms, misses, reaction times	Probe	Mind-State (MS)	$X \sim 1 + \text{Task} + (1   \text{Subject})$	$X \sim 1 + \text{Task} + \text{MS} + (1   \text{Subject})$
2d	Vigilance Scores, Pupil Size	Probe	Mind-State (MS)	$X \sim 1 + \text{Task} + (1   \text{Subject})$	$X \sim 1 + \text{Task} + \text{MS} + (1   \text{Subject})$
N/A	Vigilance Scores	Probe	SW Density (SWD; average across electrodes)	$X \sim 1 + \text{Task} + (1   \text{Subject})$	$X \sim 1 + \text{Task} + \text{SWD} + (1   \text{Subject})$
N/A	Vigilance Scores	Probe	SW Amplitude (SWA; average across electrodes)	$X \sim 1 + \text{Task} + (1   \text{Subject})$	$X \sim 1 + \text{Task} + \text{SWA} + (1   \text{Subject})$
N/A	Vigilance Scores	Probe	SW Slope (SWS; average across electrodes)	$X \sim 1 + \text{Task} + (1   \text{Subject})$	$X \sim 1 + \text{Task} + \text{SWS} + (1   \text{Subject})$
3c	Slow Wave Density (SWD); Amplitude (SWA); Slope (SWS)	Probe	Mind-State (MS)	$X \sim 1 + \text{Task} + (1   \text{Subject})$	$X \sim 1 + \text{Task} + \text{MS} + (1   \text{Subject})$
4a*	false alarms, misses, reaction times	Trial	Local Sleep (LS; per electrode)	$X \sim 1 + \text{Task} + (1   \text{Subject})$	$X \sim 1 + \text{Task} + \text{LS} + (1   \text{Subject})$
4b*	Slow Wave Amplitude (SWA); Slope (SWS)	Probe	Local Sleep (LS; per electrode)	$X \sim 1 + \text{Task} + (1   \text{Subject})$	$X \sim 1 + \text{Task} + \text{LS} + (1   \text{Subject})$
5*	a, t, z, vGo, vNoGo, vBias	Subject	Local Sleep (LS; per electrode)	$X \sim 1 + \text{Task} + (1   \text{Subject})$	$X \sim 1 + \text{Task} + \text{LS} + (1   \text{Subject})$

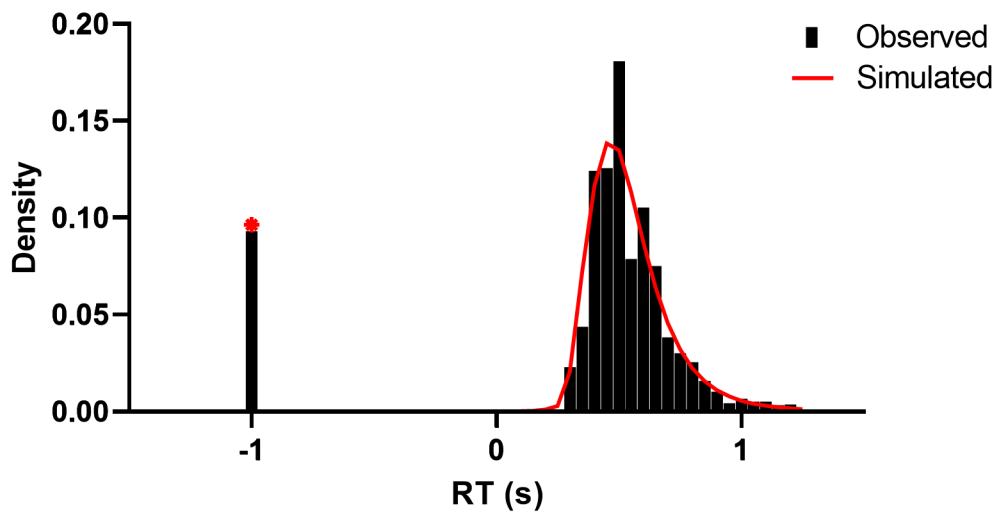
129

130 \*: Analyses corrected for multiple comparison (see Online and Supplementary Methods)..



134 **Supplementary Figure 1. Hierarchical Drift Diffusion Modelling**

135 **a:** The Go/NoGo tasks were modelled according to the Drift Diffusion Model (DDM, see  
 136 Online and Supplementary Methods). The following parameters were fitted: threshold ( $a$ ), non-  
 137 decision time or NDT ( $t$ ), bias ( $z$ ), drift rate for Go trials ( $v_{GO}$ ), drift rate for NoGo trials ( $v_{NoGo}$ )  
 138 and drift bias ( $abs(v_{GO})-abs(v_{NoGo})$ ). The figure shows a graphical representation of these  
 139 parameters. Note that here, drift rates for NoGo trials are negative. **b-c:** Graphical  
 140 representation of decision processes using the parameters obtained by the DDM for trials with  
 141 (LS+) or without (LS-) local sleep. Local sleep was defined as the presence of slow waves on  
 142 electrodes FCz (b; frontal) and Oz (c; posterior). Note the reduction in decision threshold, drift  
 143 rates and bias associated with local sleep but the increase in NDT.



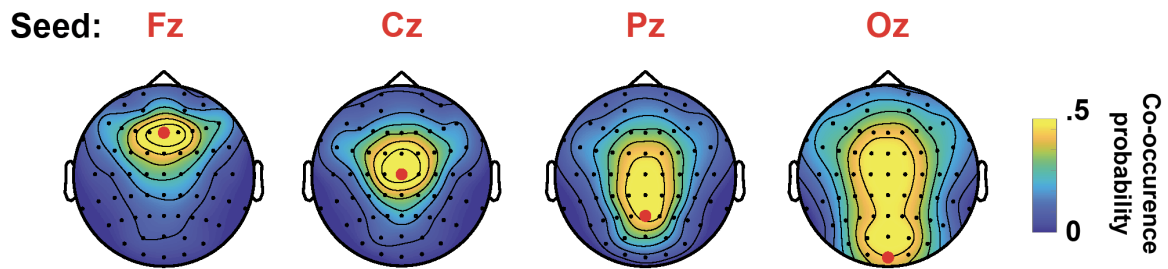
145

146 **Supplementary Figure 2. Hierarchical DDM Fit to Behavioral Data**

147 *Posterior predictive checks of Go/No-Go DDM fit to the behavioural data. Observed data*  
 148 *(black bars) are plotted underneath model-predicted RT distributions and No-Go choice*  
 149 *proportions (red lines). Positive distribution represents the normalised frequency of reaction*  
 150 *times (RT) from Go responses. Negative bin at RT=-1 represents the proportion of No-Go*  
 151 *responses.*



152



153

154 **Supplementary Figure 3. Spatial expanse of local sleep events**

155 *Four seeds electrodes were selected along the scalp midline from the front (Fz) to back (Oz).*  
156 *For each local sleep event (slow wave) detected in these seed electrodes, we computed the*  
157 *probability that local sleep was also observed in the other channels. The average co-*  
158 *occurrence probability averaged across participants (N=26) is shown for each seed electrode.*  
159 *Note that slow waves detected over Fz tend to co-occur with other local sleep events in a limited*  
160 *number of neighboring channels whereas occipital local sleep (Oz) tend to co-occur with local*  
161 *sleep events in both frontal and posterior electrodes (more widespread).*  
162